iodine isotopes suggest two rather different processes for the neutron-rich and deficient products. The recoil properties of the neutron-deficient iodine isotopes suggest a fast breakup process that may be correlated with fragment production, e.g., $Na^{24}$. Our $I^{123}$ results and the $Na^{24}$ results of Crespo can be correlated by a fast breakup process in which the light fragment shows a stronger forward peaking than the heavy.

ACKNOWLEDGMENTS

We wish to thank G. Friedlander, E. K. Hyde, and L. Yaffe for helpful discussions and critical reading of the manuscript. For chemical analyses, we are indebted to the analytical chemistry group under the direction of E. Huffman. One of us (C. B.) acknowledges fellowship assistance from the Rotary Foundation and a grant from the Fulbright Commission.

PHYSICAL REVIEW VOLUME 129, NUMBER 4 15 FEBRUARY 1963

# Experimental Investigation of Pion Electroproduction*

L. N. HAND†
*High-Energy Physics Laboratory, Stanford University, Stanford, California*
(Received 24 September 1962)

Measurements of the total cross section for the processes $e+p \rightarrow e'+n+\pi^+$ and $e+p \rightarrow e'+p+\pi^0$ are reported for a wide range of center-of-mass energies and momentum transfers extending above the first pion-nucleon resonance and to momentum transfers of 20 $F^{-2}$. Only the final electron is observed in this experiment.

Results are analyzed in terms of nucleon form factors using experimental pion-nucleon phase shifts and the theory of Fubini, Nambu, and Wataghin. In general, the data seem consistent with current picture of nucleon structure, except for a preference for a negative rather than positive neutron-electric form factor, $G_{En}$. It is demonstrated from the electron angular distribution for constant momentum transfer and constant center-of-mass energy that pion electroproduction does in fact occur primarily through transverse currents. The general form of the separation into transverse and scalar photons for inelastic or elastic electron scattering is discussed. In addition, an approximate formula for the background process of wide-angle bremsstrahlung is quoted which appears to be accurate to 1–2% over a very wide range of electron and photon energies when compared to a numerical computation by a digital computer.

## I. INTRODUCTION

THE production of single $\pi$ mesons by inelastic scattering of high-energy electrons from protons affords an indirect method for determination of the electric and magnetic structure of the neutron complimentary to that furnished by other experiments, particularly those on the electrodisintegration of the deuteron.[1,2] In particular, the direct production of mesons by electrons is sensitive to different combinations of the isotopic form factors and can, in principle, distinguish ambiguities in the sign of $F_{1n}$ arising from multiple intersections of the ellipses used in the analysis of the deuterium data.[3] The electroproduction reaction in which the energy and angle of the final-state electron are determined was first observed experimentally by Panofsky and Allton[4] and later by Ohlsen.[5] Experimental procedures for subtracting the effect of competing processes were developed by the former authors and the results interpreted in terms of a "radius" for the neutron's magnetic-moment distribution, derived from a Pauli anomalous-moment form factor assumed to be of the form:

$$F_{2n}=1/(1+r_n^2q^2/12)^2, \quad F_{1n}=0. \tag{1}$$

Here $q^2$ is the four-momentum transfer [$q^2>0$, see Eq. (3) below] and $r_n$ is the rms radius of the anomalous magnetic-moment distribution. In previous papers, exponential distributions for the two proton form factors, which also enter the theory, were assumed and $F_{1p}$ was taken as equal to $F_{2p}$.

Information gained from more recent measurements,[2,6] both for quasi-elastic scattering from the deuteron and elastic scattering from the proton, is now sufficient to permit refinement of these assumptions. In particular, it is known that $F_{1p} \neq F_{2p}$, even at $q^2=3$ $F^{-2}$. It then becomes of interest to extend the measurements of pion electroproduction over a wide range of center-of-mass energies at a fixed $q^2$ to establish the consistency of the theory of this reaction with the picture of proton and neutron structure developed from other experiments.

* This work was supported in part by the joint program of the Office of Naval Research, the U. S. Atomic Energy Commission and the Air Force Office of Scientific Research.
† Now at Harvard University, Cambridge, Massachusetts.
[1] C. de Vries, R. Hofstadter, and R. Herman, Phys. Rev. Letters **8**, 381 (1962).
[2] F. Bumiller, M. Croissiaux, E. Dally, and R. Hofstadter, Phys. Rev. **124**, 1623 (1961).
[3] C. de Vries, R. Hofstadter, R. Herman, and S. Krasner, *Proceedings of the Aix-en-Provence International Conference on Elementary Particles, 1961* (Centre d'Etudes Nucleaires de Saclay, Seine-et-Oise, 1961), Vol. 1, p. 121.
[4] W. K. H. Panofsky and E. A. Allton, Phys. Rev. **110**, 1155 (1958).
[5] G. G. Ohlsen, Phys. Rev. **120**, 584 (1960).
[6] P. Lehmann, R. Taylor, and R. Wilson, Phys. Rev. **126**, 1183 (1962).

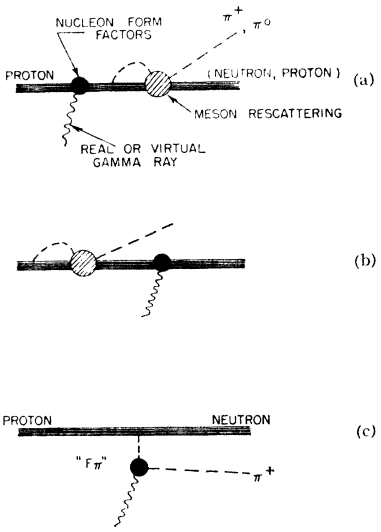


FIG. 1. Schematic representation of theoretical picture of pion electroproduction.

In order to compare this experiment with the elastic and quasi-elastic scattering experiments, it is convenient to adopt the helicity form factors first introduced by Yennie, Lévy, and Ravenhall[7] and later discussed in terms of the helicity representation[8] by Durand.[9] A preliminary discussion of the analysis of the current data on nucleon structure in terms of these form factors appears in the paper by Hand, Miller, and Wilson,[10] It is now felt that the error on $G_{En}$ implied in this last reference is too small and that the uncertainty in these quantities stems mostly from the fact that previous experiments have yielded almost no information on the neutron charge structure ($G_{En}$) beyond an upper limit on $G_{En}^2$ of about 0.1. In terms of the more commonly used $F_1$ and $F_2$ ($\kappa$ is the anomalous magnetic moment):

$$G_E=F_1-(\kappa q^2/4M^2)F_2, \quad G_M=F_1+\kappa F_2,$$
$$G_{ES}=\tfrac{1}{2}(G_{Ep}+G_{En}), \quad G_{EV}=\tfrac{1}{2}(G_{Ep}-G_{En}), \text{ etc.} \tag{2}$$

At forward angles in elastic scattering the combination $G_E^2+(q^2/4M^2)G_M^2$ is determined and at backward angles $G_M^2$ alone. In the deuterium measurements one measures essentially $d\sigma_p/d\Omega+d\sigma_n/d\Omega$ and $G_{En}^2$ is very sensitive to errors in either the cross section or the final-state corrections, because large subtractions are involved. Some estimates of the current uncertainty in the $G$'s from other experiments is given in Sec. IX below.

Pion electroproduction, on the other hand, depends on a coherent mixture of neutron and proton form factors and should provide completely independent information about the nucleon structure (see Fig. 1). The well-known $P_{3/2}$ resonance is excited through a matrix element proportional to $G_{MV}$, but other terms contain $G_{ES}$ and $G_{EV}$ and could in principle be used to resolve the ambiguity in the sign of $G_{En}$. Although the Fubini-Nambu-Wataghin[11] adaptation (FNW) of the work by Chew, Low, Goldberger, and Nambu[12] on pion photoproduction is not really satisfactory in many ways, it was found that the use of experimental phase shifts gave an excellent fit to $\pi^0$ total photoproduction cross sections over the center-of-mass energy range covered in this experiment and predicted cross sections 10–15% too high for $\pi^+$ photoproduction over the same range. Until the more ambitious work by Dennery[13] is reduced to numerical form, the FNW theory must be used. Since this experiment measures the sum of total cross sections for $\pi^0$ and $\pi^+$ electroproduction, we might expect, for low $q^2$, that the calculation used here would predict a cross section 5–8% *higher* than that actually measured (in the region corresponding to the first pion-nucleon resonance). Additional corrections of order $q^2/MK$ as described by Gartenhaus and Lindner[14] would be manifested as a progressively increasing shift of the resonance peak with increasing $q^2$ [$K$ is the equivalent photon energy; see Eq. (4) below]. Small shifts of the peak toward higher $K$ were found for $q^2=8$ F$^{-2}$ and $q^2=12$ F$^{-2}$.

With sufficient statistical accuracy, the shape of the pion-nucleon resonance can yield both $G_{En}$ and $G_{Mn}$ from this experiment alone. Such accuracy was unfortunately not attained, but it is felt that coverage of the entire resonance is essential to an understanding of the limitations in the theoretical interpretations of this type of experiment. If the data for a wide range of center-of-mass energies are combined for the form-factor analysis, the effect of uncertainties in the energy dependence of the phase shifts used in the analysis will be diminished.

For $q^2=2$, 5, 8, 12 F$^{-2}$, cross sections over center-of-mass energies covering the region of the first resonances are reported below. At $q^2=2.0$ F$^{-2}$, the measurements extend, with poorer statistical accuracy, up to the region of the second pion-nucleon resonance. No theoretical treatment is yet available for these higher center-of-mass energies. Corresponding to the peak of the first resonance, cross sections were also measured for $q^2=10$, 14, 16, and 20 F$^{-2}$. In addition a search was made for the excitation of mesons by scalar photons—a process having no counterpart in meson photoproduction. This was done by observing the angular dependence of

[7] D. R. Yennie, M. M. Lévy, and D. G. Ravenhall, Rev. Mod. Phys. **29**, 144 (1957).
[8] M. Jacob and G. C. Wick, Ann. Phys. (N. Y.) **7**, 404 (1959).
[9] L. Durand, III, *Lectures in Theoretical Physics* (Interscience Publishers, Inc., New York), Vol. 4; L. Durand, III, P. C. DeCelles, and R. B. Marr, Phys. Rev. **126**, 1882 (1962).
[10] L. N. Hand, D. G. Miller, and R. Wilson, Phys. Rev. Letters **8**, 110 (1962).
[11] S. Fubini, Y. Nambu, and V. Wataghin, Phys. Rev. **111**, 329 (1958).
[12] G. Chew, F. Low, M. Goldberger, and Y. Nambu, Phys. Rev. **106**, 1345 (1957).
[13] P. Dennery, Phys. Rev. **124**, 2000 (1961).
[14] S. Gartenhaus and C. N. Lindner, Phys. Rev. **113**, 917 (1959).

$d^2\sigma/d\Omega dE$ holding constant both $q^2$ and the center-of-mass energy. The results are consistent with the expected dominance of transverse currents in the reaction.

## II. KINEMATICS OF ELECTRON SCATTERING

In what follows, $\theta$ will be the electron-scattering angle, $\epsilon$ and $\epsilon'$, respectively, the initial and final energies of the electron. The four-momentum transfer, $q^2$, is given by (for $\epsilon$, $\epsilon' \gg 0.51$ MeV)

$$q^2 = 2\epsilon\epsilon'(1-\cos\theta). \tag{3}$$

The total energy of the reaction products in their center-of-mass system is denoted by $E$. For elastic scattering $E=M$, the proton rest mass. The threshold for meson production is $E=M+\mu$, where $\mu$ is the pion rest mass. It is found more convenient to define a new variable $K$:

$$K=(E^2-M^2)/2M, \quad \epsilon-\epsilon'=K+q^2/2M. \tag{4}$$

$K$ is the laboratory photon energy producing a final state of total center-of-mass energy $E$ upon absorption by a proton at rest. The use of $K$ as a variable eases the comparison of the electroproduction data with photoproduction. For elastic scattering $K=0$, and the threshold for meson production is $K\approx 145$ MeV. As in photoproduction, the first resonance peak is located at $K\approx 320$ MeV.

## III. SEPARATION OF TRANSVERSE AND SCALAR MATRIX ELEMENTS FOR ONE-PHOTON EXCHANGE[15,16]

The exchange of a single virtual photon between the scattered electron and the nucleon, leading to any final state, implies the following, as consequences of the vector nature of the photon:

1. There is no interference between matrix elements arising from scalar-photon absorption and transverse-photon absorption, if there is no attempt to observe the final state other than the electron. ("Transverse" and "scalar" refer to the matrix elements of the nuclear transition current in the "brick-wall" frame defined here by a Lorentz transformation along the direction of the momentum transfer, such that in this frame the electron has the same energy after the reaction as before.)

2. It is therefore possible to define total cross sections for the absorption of transverse photons and scalar photons in a manner analogous to that in photoproduction and to separate out those factors pertaining to the electron lines alone:

$$d^2\sigma/d\Omega d\epsilon = \Gamma_{\text{transverse}}(\theta,q^2,K)\sigma_{\text{transverse}}(q^2,K) + \Gamma_{\text{scalar}}(\theta,q^2,K)\sigma_{\text{scalar}}(q^2,K),$$

$$\Gamma_{\text{transverse}} \equiv \frac{\alpha}{4\pi^2}\frac{K}{q^2}\frac{\epsilon'}{\epsilon}\left[2+\frac{\cot^2(\theta/2)}{1+q_0^2/q^2}\right], \tag{5}$$

$$\Gamma_{\text{scalar}} \equiv \frac{\alpha}{4\pi^2}\frac{K}{q^2}\frac{\epsilon'}{\epsilon}\frac{\cot^2(\theta/2)}{1+q_0^2/q^2},$$

and the $\sigma$'s are defined in terms of the nuclear transition current in a manner identical to that of photoproduction, thus having the dimensions cm$^2$. The $\Gamma$'s have the dimensions: No. virtual photons/MeV-sr. The factor $(1+q_0^2/q^2)^{-1}\cot^2(\theta/2)$ is just $\cot^2(\theta^*/2)$, $\theta^*$ being the scattering angle in the brick-wall frame, and $q_0$ is the laboratory-frame energy loss of the incident electron. In the calculated cross sections as plotted later in this paper, an additional factor $|\mathbf{K}|/K$ is multiplied into the $\Gamma$'s and divided out of the $\sigma$'s, $|\mathbf{K}|$ being the laboratory momentum of the virtual photon. This different definition of the $\Gamma$'s and $\sigma$'s was used to offset the kinematic variation of the matrix elements with $q^2$ but is not recommended for future use.

The transverse-scalar separation is perfectly general and should have applications even when the electron is virtual. For example, in pair production from targets with $Z>1$, one is freed in principle from any nuclear physics calculations, since the cross section, in the one-photon exchange approximation, must separate into the sum of two functions, each measurable by appropriate electron-scattering experiments.

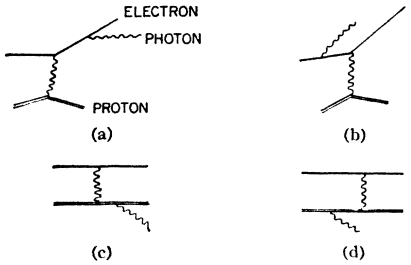


FIG. 2. Feynman diagram for wide-angle bremsstrahlung.

## IV. EXPERIMENTAL METHOD

There are several reactions also leading to energy-degraded electrons at large angles. The most prominent of these is wide-angle bremsstrahlung (Fig. 2). Other reactions include the Coulomb scattering of knock-on electrons from electron-electron scattering, wide-angle pair and trident production (at small angles), and electrons resulting from either external or internal (Dalitz pairs) conversion of gamma rays from $\pi^0$ decay, or from $\mu^\pm$ decay. Panofsky and Allton showed that all of the above background reactions (except *e-e* scattering—see reference 4) necessarily involve the radiation of a high-energy photon by an electron either in the Coulomb

[15] This separation of the matrix elements for the particular case of single-pion production was first derived by R. H. Dalitz and D. R. Yennie, Phys. Rev. **105**, 1598 (1957) and for elastic electron scattering in reference 7.

[16] L. N. Hand, Ph.D. thesis, Stanford University, 1961 (unpublished). M. Gourdin, Nuovo Cimento **21**, 1094 (1961).

field of the proton participating in the reaction (virtual radiator) or in the physical radiator elsewhere in the target. Because the amount of virtual radiator is largely independent of the process involved, it is possible to eliminate the competing processes by extrapolating the observed counting rate, as a function of additional radiator, to zero radiator including the virtual radiator. This is the "radiator subtraction" method used by Panofsky-Allton and Ohlsen. This procedure was not followed in this experiment for two reasons:

1. The extrapolation greatly degenerates the statistical accuracy, particularly away from the resonance.

2. The conclusion drawn by Panofsky[4] regarding the elimination of the wide-angle bremsstrahlung by radiator subtraction was based on a calculation by Schiff[17] valid in the limit of infinite proton mass. Magnetic-moment scattering and recoil effects are quite important in the energy and angular region of this experiment. Furthermore, Panofsky advances physical reasons for the results of Schiff's calculation which prove, upon actual calculation,[16] to be somewhat misleading. He argues that the integration over direction of the final-state gamma ray greatly favors the emission of the gamma ray either along the direction of the incident electron or the direction of the final electron hence leading to a virtual intermediate electron which is nearly real in either Fig. 2(a) or (b) for gamma rays collinear with the initial or final electrons, respectively. These two states being quite different, Panofsky argues that they do not interfere and that the cross section may thus be approximately factored into radiation followed by elastic scattering [Fig. 2(b)] plus elastic scattering followed by radiation [Fig. 2(a)]. One would then assume that the correct calculation would merely involve substitution of the Rosenbluth cross section for the Mott cross section and multiplication by certain kinematic factors deduced from the physical picture evoked. It is remarkable that this does in fact turn out to be substantially correct, because the major contribution to the cross section comes from the interference between the amplitudes represented in Fig. 2(a) and Fig. 2(b).[18]

The possibility of abandoning the method of "radiator subtraction" then rests on the following observations: (1) One must calculate the cross section for wide-angle bremsstrahlung even with the "radiator subtraction," and (2) several of the other background processes (see references 4 and 16) give rise to equal numbers of positrons and electrons. Thus, assuming that the predominance of $\pi^+$ mesons does not significantly augment the measured positron flux by $\pi^+ \rightarrow \mu^+ \rightarrow e^+$, charge exchange scattering in the counter, followed by gamma-ray conversion, or direct counting in the Čerenkov counter for sufficiently high-pion momenta, we may remove the contribution from the "charge symmetric" processes by subtracting the number of positives from negatives. (3) It is possible to check these assumptions by choosing $K<$pion threshold, in which case all remaining counts should be attributable to wide-angle bremsstrahlung.

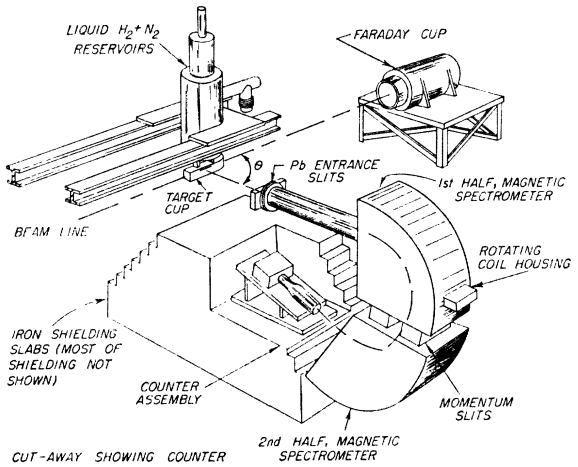


FIG. 3. Experimental arrangement with cutaway showing Čerenkov counter.

The actual data runs were three in number, separated by three weeks and three months. Measured values of elastic scattering from hydrogen, used for normalization of cross sections in the manner described in Sec. VI were taken on the first two runs and several data points were repeated to check the internal consistency of the runs. Points for $K$ below pion threshold were taken on all three runs to check the wide-angle bremsstrahlung subtraction, and the positron flux was determined for each data point separately, as were pulse-height distributions for both positive and negative settings of the magnet.

## V. APPARATUS

Figure 3 illustrates the experimental arrangemene (not to scale). The vacuum chamber surrounding tht liquid-hydrogen target cup is not shown.

Particles from the liquid hydrogen having a given direction within a small solid angle and having a momentum $p'$ are selected by the magnetic spectrometer and counted by the Čerenkov light produced as they pass through a cylinder 5 in. in diam and 10 in. long, filled with paraffin oil ($n \approx 1.5$). For a given set of data at a fixed angle $\theta$, the initial and final electron energies were chosen so that $q^2$ remained constant and $K$ was varied from an energy well below the first resonance (320 MeV) to a value limited by the upper energy limit of the linear accelerator. The incident beam was captured in a Faraday cup believed to be better than 99% efficient for energies well in excess of 600 MeV.[19] The collected charge was integrated on a condenser in a

[17] L. I. Schiff, Phys. Rev. 87, 750 (1952).

[18] D. R. Yennie has observed that this large interference term arises only if the sum over photon polarizations is performed covariantly (private communication).

[19] D. Yount (private communication).

standard feedback amplifier circuit and the voltage read with a potentiometer.

The target cup was $7\frac{1}{2}$ in. long of which about $3\frac{1}{2}$ in. was within the acceptance profile of the spectrometer at 90°. The lead entrance slits further reduced the possibility that an electron originating in the 2-mil Dural entrance window of the target cup or the 7-mil aluminum vacuum chamber window would pass through the spectrometer. The counting rate with the liquid hydrogen removed was consistent with the density of the cold gas—about 1.5% of the full target rate. It is therefore assumed that only electrons from the hydrogen are counted. With the entrance slits closed, the counting rate was sufficiently small as to be completely negligible.

The electronic circuitry was completely straightforward, being a single channel integral discriminator gated on during the beam pulse. The Čerenkov counter was viewed at one end by an RCA-type 7046 photomultiplier. The two-thirds of the cylinder nearest the phototube were silvered, and the other third was blackened to increase the directionality. Most of the background in Čerenkov counters at this accelerator appears caused by low-energy electrons originating from gamma-ray interactions in the counter, the gamma rays resulting from neutron capture in the shielding or in the counter itself. Thus the energy of background electrons is necessarily less than the binding energy of neutrons in the shielding material. "Signal" electrons traversed path lengths corresponding to an energy loss for a minimum ionizing particle of more than 30 Mev before emitting light sufficient to register a count. The absolute threshold for counting pions by Čerenkov light was a momentum of 130 MeV/$c$ and for muons 100 MeV/$c$, but it was impossible to detect pions below 195 MeV/$c$ even with very much reduced discriminator bias because the pulse height is reduced due to scattering and slowing down to the paraffin oil. Above this momentum, it was possible to observe a second peak on the pulse-height spectrum. This peak was due to positive pions and increased in pulse height rapidly with respect to the position peak as the momentum was increased. From this pulse-height analysis and measurements of the cross section below electroproduction threshold, it is believed that the efficiency of the counter was negligible for pions and muons below 210 MeV/$c$. A few data points were taken for secondary particle moments greater than 210 MeV/$c$, up to 250 MeV/$c$. In this range, the efficiency for pions and muons, although small, increased rapidly, the average pulse height of a pion being 60% of that for an electron at 250 MeV/$c$. This is less than would be expected on the basis of the Čerenkov light dependence on particle velocity and is probably caused by scattering of the pions.

Only one point ($q^2=20$ F$^{-2}$) is reported here with an electron final energy of greater than 210 MeV, and hence with some possible $\pi^+$ contamination in the subtracted positive flux. For this point a measurement below threshold for electroproduction at the same angle and secondary energy ($\epsilon'=233$ MeV) was taken and the wide-angle bremsstrahlung cross section is assumed to be correct. One may then reverse the procedure followed on the other data points and calculate the addition to the positive particle counts presumably due to the residual efficiency for pions and muons. Raising the incident beam energy to that corresponding to $q^2=20$ F$^{-2}$, $K=320$ MeV does not greatly affect the number of pions, since the dominant process is single-meson production from a gamma-ray energy less than the lower of the two-incident electron energies. A small correction is applied for the change in initial energy and the number of positives corrected for meson contamination. This procedure is obviously not very satisfactory, and the errors are increased accordingly for the $q^2=20$ F$^{-2}$ point. The asymmetry in quoted errors is due to the uncertainty in this correction for meson contamination.

The pulse-height spectrum for electrons was about 20% full width at half height. The discriminator bias was set for pulses about 80% of the average pulse height for electrons with a consequent loss in efficiency for low energy (<100 MeV) electrons. Normalization by elastic electron scattering allows this loss to be measured and the necessary correction to be made (see below).

An additional source of residual efficiency for pions is the possibility of a charge exchange collision in the counter followed by conversion of the decay gamma rays. Unlike the direct counting of the pions, this effect might persist at lower pion momenta. This was estimated crudely by considering the slowing down of the entering pion, the angular distribution for charge exchange (taken to be the same as $\pi^-$ on protons), the $\pi^0$ decay kinematics, etc. A threshold of 30 MeV loss for one $e^+-e^-$ pair in the counter was assumed. The estimated efficiency increases rapidly with pion momentum: For momenta of 250 MeV/$c$, 175 MeV/$c$, and 135 MeV/$c$, the estimated efficiency for pion detection from charge exchange is 0.06%, 0.03%, and 0.01%, respectively. Except at 250 MeV/$c$, this is completely negligible, and, at the higher momentum, it is also subtracted by use of the threshold data, as described above.

Decay of muons in flight is estimated to give a negligible contribution to the electron flux at these momenta. Counts delayed up to several microseconds after the beam were observed, when the spectrometer was set for positives at a momentum sufficiently low to permit the pions to stop in the counter. These late counts were most prevalent for $\approx$160 MeV/$c$ corresponding to a pion range almost equal to the full length of the counter, and increased with lower discriminator setting. The late counts are attributed to electrons from $\mu^+$ decay. Almost no late counts were observed for negative particles passing through the counter. A correction for prompt recording of these decays was applied, assuming a flat beam pulse of 0.6 $\mu$sec length and using the counts recorded in three time intervals covering a total of

7 $\mu$sec after the beam pulse. The correction was never very large, being at most 15% of the positive rate. Small corrections ($<2\%$) for positron annihilation in the counter and for counting rate losses were also made.

## VI. NORMALIZATION

In order to convert the number of counts per volt on the integrating capacitor to a cross section for inelastic electron scattering, it is necessary to know the product of the counter efficiency and the phase-space acceptance of the spectrometer. The latter was a double focusing, zero-dispersion spectrometer described by Alvarez, Brown, Panofsky, and Rockhold.[20] The momentum acceptance was maintained at a nominal $\Delta p'/p'=2\%$. Since a continuum of scattered energies is being measured, it would be most convenient to use a precisely measured continuum cross section as an absolute reference. This, however, is not available, but it is possible to simulate this continuum by observing *elastic* scattering from the hydrogen and varying the incident beam energy, so that the scattered electron energies span the momentum acceptance of the spectrometer. This method was suggested by Richter and used by Panofsky and Allton.[4] The chief complication involves a proper treatment of the effect of the radiative degeneration of electron energy, an effect only estimated in reference 4. If radiation of low-energy photons did not take place, then the conversion factor from counts per integrated volt to inelastic cross section, $d^2\sigma/d\Omega d\epsilon'$ (referred to below as the "phase-space integral"), is given by the ratio:

$$\sum_i \frac{C_0(\epsilon_i,\epsilon')\Delta\epsilon_i\, d\epsilon'}{d\sigma/d\Omega(\epsilon_i,\theta)\, d\epsilon_i} = \frac{C_I}{1.602\times10^{-9}} N_H f(\epsilon')\epsilon' \int dZ\left[\frac{\Delta\epsilon'}{\epsilon'}\right]_Z \Delta\Omega,$$

where $C_0(\epsilon_i,\epsilon')$ = counts per integrated volt on capacitor with spectrometer set for energy $\epsilon'$ and incident beam energy $\epsilon_i$, $\Delta\epsilon_i$ = spacing between incident energy steps, $d\epsilon'/d\epsilon$ = recoil factor for elastic scattering = $(\epsilon'/\epsilon)^2$, $d\sigma/d\Omega(\epsilon_i,\theta)$ = elastic scattering cross section for electrons from protons, $C_I$ = integrating capacitance in farads, $N_H$ = number of protons/cm$^3$ in target, $dZ$ = incremental distance along beam in hydrogen target, and $f(\epsilon')$ = efficiency of counter.

The counter efficiency varied somewhat with energy, especially for $\epsilon'<100$ MeV, because the discriminator bias was set high to reduce the sensitivity to pions when counting positrons and to eliminate empty target background. Along with the neglect of radiative effects, the above formula is derived under the assumption that the width of the incident-beam-energy spectrum is narrow compared to $\Delta p'/p'$ for the spectrometer. The nominal width of the beam spectrum was set at $\frac{1}{4}\%$. It can be shown[16] that corrections from the finite width $\Delta\epsilon$ of the incident spectrum are proportional to $(\Delta\epsilon/\Delta\epsilon')^2$ and in any case tend to cancel in the integral defined above.

The effect of radiation upon the observed spectrum $C_\delta(\epsilon_i,\epsilon')$ is treated by an iterative procedure using a digital computer. An integral equation is easily written to describe the effect of radiative degeneration upon the observed spectral shape and the computer calculates the correction for each value of $C_\delta(\epsilon_i,\epsilon')$, using the difference between the observed spectrum and a fold of the hypothetical radiation-free spectrum $C_0(\epsilon_i,\epsilon')$ with the theoretical radiative tail. As a first approximation to $C_0$, $C_\delta$ is used. Since the number of radiation lengths (virtual plus real) in the beam is $\approx0.03$, the process converges rapidly.

$$C_\delta(\epsilon_i,\epsilon')=C_0(\epsilon_j,\epsilon')R_{ij\epsilon_i}\leq\epsilon_j, \text{ summed over } j.$$

$R_{ij}$ is given approximately by the expression

$$\exp\{-\delta\ln[\epsilon_j/(\epsilon_j-\epsilon_i+\tfrac{1}{2}\Delta\epsilon)]\} - \exp\{-\delta\ln[\epsilon_j/(\epsilon_j-\epsilon_{i-1}+\tfrac{1}{2}\Delta\epsilon]\},$$

where $\delta$ is the sum of the number of real radiation lengths ahead of the scattering event and the virtual radiator as calculated by Tsai.[21] $\Delta\epsilon$ is the spacing of incident energy steps. In the actual calculation, a correction was made for the fact that some of the scattering takes place at a lower energy, corresponding to soft-photon radiation in the direction of the incident beam. No correction for the possibility that the recoiling proton might radiate a soft photon was made. This is believed $<2\%$ for low-momentum transfers to the proton. For the details of the above calculation see reference 16. This procedure was checked in two ways. The phase-space integral was computed for a spectrum obtained by Allton (under slightly different experimental conditions) with and without an additional 0.05 radiation length of copper added ahead of the target. The observed spectra appear quite different, but the unfolded $C_0(\epsilon_i,\epsilon')$ are essentially identical, and the phase-space integrals given by Eq. (6) agree to 1%. Such good agreement is probably fortuitous. The phase-space integrals calculated as in reference 4, in which radiative effects are only estimated, differed by about 10%. The additional radiator corresponds to a much more extreme condition than normally encountered, and one might estimate the error in the more approximate method given by Panofsky and Allton to be about 5% with 0.03 radiation length effective. Another check is the absence of a radiative tail on the unfolded spectrum. In actual practice, this tail was not quite completely removed. The residual amount was not always positive and may represent the effect of finite resolution or of statistical fluctuations in the counts on the unfolding procedure. About 3% of the total area was included in

[20] R. A. Alvarez, W. K. H. Panofsky, and C. T. Rockhold, Rev. Sci. Instr. **31**, 556 (1960).

[21] Y. S. Tsai, Phys. Rev. **122**, 1898 (1961).

TABLE I. Normalization from elastic electron scattering.

| $\theta$ | $\epsilon'$ (MeV) | Phase space[a] | Normalized phase space[a] |
|---|---|---|---|
| 90° | 211 | 24.2 | 11.5 |
| 135° | 151 | 16.0 | 10.6 |
| | 91 | 8.45 | 9.26 |
| 135° | 210 | 34.3 | 11.5 |
| | 181 | 28.9 | 11.3 |

[a] See text for units.

this tail. This is probably a measure of the accuracy of the normalization procedure, assuming perfect knowledge of the elastic-scattering cross sections.

For the measurement of the product of phase space times counter efficiency, five points were selected (Table I), corresponding to momentum transfers at 90° of 2.9, 1.4, and 0.47 $F^{-2}$ and at 135° to 6.3 and 3.2 $F^{-2}$. The elastic-scattering cross section was calculated using an exponential model with a radius equal to 0.80 F and setting $F_{1p}=F_{2p}$.[3] The effect of the recent, more accurate knowledge of the form factors ($F_{1p}\neq F_{2p}$, even for low $q^2$) on these particular points is slight, being of order 3% or less. The column labeled "phase space" in Table I gives the conversion factor at that angle and energy in units of counts per 100 V integrated on a condenser with a nominal value of $10^{-6}$ F for a cross section of $10^{-35}$ cm$^2$/MeV-sr. "Normalized phase space" is a measure of counter efficiency and at 211 MeV for 90° and 135° the consistency of the normalization procedure. These numbers equal the phase-space factor corrected for the expected proportionality to $\epsilon'$ and inverse proportionality to $\sin\theta$, due to the change in effective target length. The drop of 20% in counter efficiency for very low energy electrons can also be estimated from the pulse-height distribution and the known cutoff point for the discriminator, also observed with the pulse-height analyzer. The efficiency thus estimated is in agreement with the above table. This efficiency loss is undoubtedly caused by multiple scattering of the electrons out of the counter, before they have emitted sufficient Čerenkov light to record a count. A correction was applied to the data by estimating the efficiency range for energies other than those measured directly using an empirical curve (quadratic) fitted to the observed relative efficiencies at 210, 180 and 150 MeV, for energies above 150 MeV and a linear fit to the observed relative efficiency between 90 and 150 MeV. The correction applied at 180 MeV was 2% relative to 210 MeV, at 150 MeV 8.5% and at 90 MeV 24%. The largest correction affects points with lowest secondary energy, i.e., points corresponding to very high $K$, or center-of-mass energy, at the lowest $q^2$ values. These points already have large errors, because the wide-angle bremsstrahlung dominates the observed secondary flux, but the errors should probably be increased somewhat because of the uncertainty in the efficiency correction. A few points were taken at a lower discriminator setting to lessen this uncertainty, and the correction applied here reached a maximum of 10% at the lowest energies, as estimated from the pulse height distribution and from ratios taken with elastically scattered electrons. No inconsistencies were observed between points taken at the two different settings after these corrections were made, within the errors to be quoted. A further check of these procedures comes from the wide-angle bremsstrahlung measurements below pion-production threshold, as discussed below.

Elastic-scattering spectra at energies identical to those in Table I were observed at various times throughout the experiment to check that no shifts in the energy calibration or counter efficiency occurred.

## VII. WIDE-ANGLE BREMSSTRAHLUNG

As mentioned in the introduction, the major source of noncharge symmetric background arises from the process of wide-angle bremsstrahlung. Because the physical argument advanced by Panofsky had actually only been proved in the limit of infinite proton mass[17] and because it was known that in the very similar calculation of wide-angle pair production by Bjorken, Drell, and Frautschi[22] that the interference terms were dominant, the wide-angle bremsstrahlung (WAB) process was calculated directly from the Feynman diagrams of Fig. 2 in the approximation that the variation of the numerators can be neglected near the photon angles for which the denominator becomes small and that these regions dominate the cross section. In this approximation (called the "peaking approximation") it was possible to see that the factorization described by Panofsky does in fact occur, the cross section for wide-angle bremsstrahlung being given by the expression: (denote by $E_2$ the final electron energy, $E_1$ the initial electron energy)

$$\left(\frac{d^2\sigma}{d\Omega dE_2}\right)_{\mathrm{WAB}}=\eta_1^2\frac{X_1}{k_1}\frac{d\sigma}{d\Omega}(\theta,E_1)+\frac{X_2}{k_2}\frac{d\sigma}{d\Omega}(\theta,E_1') \quad (7)$$

with $d\sigma/d\Omega(\theta,E)$=Rosenbluth cross section for elastic scattering at an angle $\theta$ and an energy $E$, $\eta_1$=recoil factor if electron radiates before scattering;

$$\eta_1=1/[1-E_2(1-\cos\theta)/M]=E_1'/E_2,$$
$$k_1=E_1-E_1'\neq k_2=E_2'-E_2,$$

and

$$E_1'=E_1/[1+E_1(1-\cos\theta)/M].$$

$X_1$ and $X_2$ are the equivalent radiation lengths for radiation before and after scattering, respectively:

$$X_{1,2}=-\frac{\alpha}{\pi}\frac{\eta_{1,2}}{\eta}\left[\ln\left(\frac{q^2}{m^2}\right)-1+\frac{k_1^2}{E_{1,2}E_{1,2}'}\ln\frac{2E_{1,2}}{m}\right]. \quad (8)$$

[22] J. D. Bjorken, S. D. Drell, and S. C. Frautschi, Phys. Rev. 112, 1409 (1958).

The arguments of the logarithms are only approximate, but agree with Tsai's formula as $k_1$, $k_2 \rightarrow 0$. $\eta = E_1/E_2$, and $m$ is electron mass. The recoil factor for radiation before scattering and $1/k_1$ or $1/k_2$ in the above is exactly the intuitively correct expression for this cross section also found by Tsai, but in the limit $k \rightarrow 0$. Berg and Lindner have made a more exact calculation of this process[23] which has been extensively checked and programed for the computer by Allton, since the above calculation was made. In comparing the result from this formula with the more exact computer program, the effect of proton bremsstrahlung is believed to be $<1\%$ and was neglected. Numerical results from the Berg-Lindner calculation of proton bremsstrahlung should be available soon.[24] Under these assumptions, the agreement between the above formula and the numerical integration of the Berg-Lindner formulas for radiation by the electron proved to be suprisingly good, being within 1 or 2% for center of mass energies near or below meson production threshold, 2 or 3% near the first resonance and increasing for higher equivalent photon energies because the low secondary electron energy increasingly invalidates the accuracy of the approximation made in deriving Eq. (8).

TABLE II. Calculated and experimental inelastic cross sections below pion threshold ($K=120$ MeV). (Cross sections in units of $10^{-35}$ cm$^2$/MeV-sr.)

| $\epsilon'$ (MeV) | $\theta$ | $\sigma^-$ | $\sigma^+$ | $(\sigma^- - \sigma^+)$ | Calculated WAB |
|---|---|---|---|---|---|
| 140.0 | 135° | 3.03 ±0.17 | 0.933±0.16 | 2.10 ±0.24 | 2.31 |
| 174.5 | 60° | 63.1 ±1.7 | 1.33 ±0.25 | 61.8 ±1.7 | 52.9 |
| 175.0 | 135° | 1.89 ±0.09 | 0.287±0.06 | 1.60 ±0.11 | 1.42 |
| 209.4 | 135° | 0.903±0.073 | 0.206±0.045 | 0.696±0.086 | 0.826 |
| 210.0 | 90° | 5.56 ±0.48 | 1.15 ±0.22 | 4.40 ±0.53 | 4.85 |

An overall error was assigned to the calculated value of the wide-angle bremsstrahlung cross section equal to 10% for the 60° points ($q^2=2$ F$^{-2}$) and 5% for all other points. This error was then propagated into the errors assigned to the pion electroproduction cross sections. Near the first pion-nucleon resonance it had little

TABLE III. Pion electroproduction data. $\theta=60°$ (except as noted). $q^2=2.0$ F$^{-2}$.

| $K$ (MeV) | $\sigma^-$ | $\sigma^+$ | WAB (10% error assigned) | $d^2\sigma/d\Omega dE'$ | $10^6\Gamma_{tr}'$ | $\sigma_{tr}$ ($\mu$b) |
|---|---|---|---|---|---|---|
| 230 | 47.0±1.0 | 3.37±0.30 | 24.1 | 19.5±2.8 | 1.28 | 153±22 |
| 230 (90°) | 28.2±0.99 | 5.06±0.72 | 11.8 (5% error) | 11.2±1.3 | 0.642 | 175±22 |
| 280 | 67.3±1.9 | 5.76±0.54 | 23.2 | 38.2±3.0 | 1.11 | 344±28 |
| 310 | 77.6±2.1 | 6.63±0.60 | 23.2 | 47.7±3.2 | 1.03 | 464±32 |
| 330 | 75.7±2.0 | 6.72±0.61 | 23.3 | 45.6±3.1 | 0.974 | 469±32 |
| 380 | 61.3±1.3 | 9.28±0.73 | 24.0 | 27.9±2.7 | 0.865 | 323±31 |
| 430 (45°) | 72.6±1.5 | 9.6 ±0.9 | 34.2 | 28.7±3.8 | 1.35 | 213±28 |
| 430 (75°) | 46.0±1.5 | 14.6 ±1.2 | 20.1 | 11.1±2.1 | 0.522 | 213±40 |
| 430 | 54.3±1.3 | 10.8 ±0.8 | 25.1 | 18.3±2.9 | 0.776 | 236±37 |
| 480 | 55.5±1.4 | 12.1 ±0.9 | 26.7 | 15.3±2.1 | 0.707 | 216±30 |
| 530 | 55.1±1.4 | 14.6 ±1.0 | 28.5 | 15.5±3.4 | 0.643 | 241±53 |
| 580 | 59.7±1.5 | 15.5 ±1.1 | 30.7 | 13.3±3.5 | 0.594 | 224±59 |
| 630 | 64.2±1.6 | 17.8 ±0.8 | 33.2 | 12.9±3.7 | 0.550 | 234±67 |
| 680 | 72.8±1.3 | 20.8 ±1.3 | 36.1 | 15.6±4.1 | 0.512 | 305±80 |
| 709 | 76.8±1.9 | 22.8 ±1.4 | 37.7 | 16.0±4.4 | 0.493 | 324±89 |
| 712 (45°) | 91.0±1.5 | 27.9 ±0.9 | 42.3 | 20.5±4.5 | 0.834 | 246±54 |
| 730 | 77.7±1.5 | 23.8 ±1.1 | 39.3 | 14.2±4.3 | 0.480 | 296±90 |
| 753 | 82.8±2.0 | 26.5 ±1.6 | 41.1 | 14.8±4.8 | 0.465 | 318±103 |
| 769 | 82.0±2.0 | 29.3 ±1.7 | 42.2 | 10.2±4.9 | 0.455 | 208±108 |

TABLE IV. Pion electroproduction data. $\theta=90°$ (except as noted). $q^2=5.0$ F$^{-2}$.

| $K$ (MeV) | $\sigma^-$ | $\sigma^+$ | WAB (5% error) | $d^2\sigma/d\Omega dE'$ | $10^6\Gamma_{tr}'$ | $\sigma_{tr}$ ($\mu$b) |
|---|---|---|---|---|---|---|
| 230 | 8.65±0.29 | 1.37±0.18 | 2.89 | 4.37±0.37 | 0.498 | 88 ± 7.4 |
| 230 (135°) | 5.72±0.29 | 1.49±0.21 | 1.31 | 2.90±0.37 | 0.301 | 96.4±12.3 |
| 280 | 14.1 ±0.31 | 1.93±0.18 | 2.75 | 9.45±0.39 | 0.446 | 212 ± 9 |
| 330 | 17.27±0.35 | 2.94±0.24 | 2.73 | 11.60±0.45 | 0.402 | 288 ±11 |
| 330 (135°) | 11.01±0.31 | 2.67±0.22 | 1.21 | 7.10±0.40 | 0.240 | 296 ±17 |
| 380 | 13.8 ±0.53 | 3.65±0.48 | 2.77 | 7.37±0.73 | 0.367 | 201 ±20 |
| 430 | 12.9 ±0.47 | 4.47±0.32 | 2.87 | 5.53±0.58 | 0.335 | 165 ±17 |
| 480 | 13.0 ±0.49 | 5.51±0.32 | 3.00 | 4.43±0.60 | 0.309 | 143 ±19 |
| 530 | 14.1 ±0.52 | 6.73±0.45 | 3.17 | 4.08±0.71 | 0.286 | 143 ±25 |
| 580 | 15.7 ±0.47 | 7.58±0.40 | 3.37 | 4.75±0.64 | 0.268 | 177 ±24 |
| 630 | 16.4 ±0.61 | 8.97±0.57 | 3.59 | 3.71±0.86 | 0.248 | 150 ±35 |
| 680 | 17.7 ±0.65 | 10.7 ±0.59 | 3.84 | 2.98±0.90 | 0.234 | 127 ±38 |

[23] R. A. Berg and C. N. Lindner, Phys. Rev. **112**, 2072 (1958).
[24] E. A. Allton (to be published).

TABLE V. Pion electroproduction data. $\theta=135°$ (except as noted). $q^2=8.0$ F$^{-2}$.

| $K$ (MeV) | $\sigma^-$ | $\sigma^+$ | WAB (5% error) | $d^2\sigma/d\Omega dE'$ | $10^6\Gamma_{tr}'$ | $\sigma_{tr}$ ($\mu$b) |
|---|---|---|---|---|---|---|
| 230 | 3.08±0.13 | 0.53±0.09 | 0.73 | 1.82±0.16 | 0.250 | 72.8± 6.4 |
| 230 (90°) | 3.84±0.13 | 3.72±0.21 (0.99±0.64)[a] | 1.36 | $1.49_{-0.62}^{+1.13}$ | 0.412 | $36_{-15}^{+27}$ |
| 270 | 4.54±0.19 | 0.80±0.13 | 0.69 | 2.93±0.18 | 0.232 | 126 ±8 |
| 310 | 5.88±0.19 | 1.20±0.12 | 0.66 | 3.99±0.23 | 0.215 | 186 ±11 |
| 330 | 6.64±0.19 | 1.28±0.15 | 0.66 | 4.69±0.24 | 0.207 | 226 ±12 |
| 350 | 5.65±0.19 | 1.23±0.13 | 0.65 | 3.76±0.24 | 0.201 | 187 ±12 |
| 380 | 5.38±0.23 | 1.44±0.17 | 0.65 | 3.27±0.29 | 0.190 | 172 ±15 |
| 400 | 5.15±0.18 | 2.32±0.15 | 0.65 | 2.16±0.24 | 0.185 | 117 ±13 |
| 430 | 5.31±0.27 | 2.07±0.21 | 0.65 | 2.56±0.34 | 0.176 | 145 ±19 |
| 480 | 5.33±0.28 | 2.61±0.23 | 0.66 | 2.03±0.37 | 0.163 | 125 ±23 |
| 539 | 5.67±0.28 | 3.42±0.22 | 0.67 | 1.51±0.36 | 0.15 | 100 ±24 |
| 580 | 6.02±0.32 | 3.65±0.27 | 0.69 | 1.62±0.42 | 0.143 | 113 ±29 |
| 630 | 6.91±0.36 | 4.18±0.32 | 0.72 | 1.94±0.48 | 0.134 | 145 ±36 |
| $q^2=10.0$ F$^{-2}$ | | | | | | |
| 330 | 4.44±0.17 | 0.66±0.12 | 0.48 | 3.29±0.22 | 0.19 | 173 ±12 |

[a] Corrected for meson contamination.

effect, because the wide-angle bremsstrahlung was a fraction of the counting rate. The numerical assignment of this error is based in part on the agreement between predicted and observed cross sections below meson threshold (Table II) and in part on estimates in the uncertainty in interpolations on the nucleon form factors, the radiative corrections to the wide-angle bremsstrahlung and to the effects of finite target length and finite spectrometer angular asymmetries.

Radiative corrections computed for the wide-angle bremsstrahlung were of two types, which tended to cancel each other. As in elastic scattering, a correction arises due to soft-photon emission, in addition to the single hard photon, tending to reduce the observed counts for a given initial and final electron energy by about 10–15%, depending on the particular experimental situation. Unlike elastic scattering, we may also have the emission of two moderately hard photons, with an integral over all possible combinations, i.e., over the scattering cross section (in the "peaking" approximation described above) for energies intermediate between those dominant in the case of single-photon bremsstrahlung. A numerical integral of the two-photon bremsstrahlung was performed on a computer for each case of interest and combined with the soft-photon correction. In every case the net effect was only a few percent.

As mentioned previously, electron-electron scattering is an important source of low-energy secondaries which becomes dominant for sufficiently low energies ($\epsilon'<50$ MeV) because the spectrum of $\delta$ rays has the dependence $\epsilon'^{-2}$ on secondary electron energy. In the analysis of the data, it is convenient to include this effect with the wide-angle bremsstrahlung for the case in which the hard photon is radiated before scattering. No correction was included for this effect in the event of scattering first.

The calculation of radiation lengths in the liquid hydrogen was made using a computer program kindly supplied by R. Alvarez.[25]

TABLE VI. Pion electroproduction data. $\theta=135°$. $q^2=12.0$ F$^{-2}$.

| $K$ (MeV) | $\sigma^-$ | $\sigma^+$ | WAB (5% error) | $d^2\sigma/d\Omega dE'$ | $10^6\Gamma_{tr}'$ | $\sigma_{tr}$ ($\mu$b) |
|---|---|---|---|---|---|---|
| 230 | 1.22±0.07 | 0.25±0.06 | 0.404 | 0.57±0.10 | 0.207 | 27.5± 4.8 |
| 270 | 2.06±0.12 | 0.28±0.06[a] | 0.38 | 1.4 ±0.14 | 0.193 | 72.5± 7.3 |
| 290 | 2.47±0.14 | 0.10±0.05 | 0.38 | 2.0 ±0.16 | 0.188 | 106 ± 8.5 |
| 310 | 2.99±0.16 | 0.28±0.06[a] | 0.37 | 2.34±0.17 | 0.181 | 129 ± 9.4 |
| 330 | 3.33±0.17 | 0.39±0.08 | 0.37 | 2.57±0.19 | 0.176 | 146 ±11 |
| 350 | 3.00±0.16 | 0.40±0.08[b] | 0.37 | 2.60±0.18 | 0.171 | 152 ±11 |
| 370 | 2.60±0.14 | 0.43±0.09 | 0.37 | 1.79±0.18 | 0.165 | 109 ±11 |
| 400 | 2.31±0.11 | 0.66±0.08 | 0.37 | 1.11±0.23 | 0.160 | 69.4±14 |
| 430 | 2.16±0.15 | 0.90±0.11 | 0.37 | 0.88±0.19 | 0.153 | 57.5±12 |
| 480 | 2.62±0.19 | 1.12±0.13 | 0.37 | 1.11±0.23 | 0.144 | 77.1±16 |
| $q^2=14.0$ F$^{-2}$ | | | | | | |
| 330 | 2.18±0.13 | 0.35±0.09 | 0.29 | 1.53±0.16 | 0.164 | 93.3± 9.7 |

[a] Average $\sigma^+$ for $K=230$, 290, 330.
[b] Average $\sigma^+$ for $K=330$, 370.

[25] R. Alvarez, Int. Memorandum, High-Energy Physics Laboratory, Stanford University, 1961 (unpublished).

TABLE VII. Pion electroproduction data. $\theta=135°$. $q^2=16.0$ F$^{-2}$.

| $K$ (MeV) | $\sigma^-$ | $\sigma^+$ | WAB | $d^2\sigma/d\Omega dE'$ | $10^6\Gamma_{tr}'$ | $\sigma_{tr}$ ($\mu$b) |
|---|---|---|---|---|---|---|
| 250 | 0.81±0.05 | 0.44±0.06<br>(0.22±1.0)[a] | 0.24 | 0.59±0.11 | 0.172 | 34±6.4 |
| 310 | 1.39±0.07 | 0.32±0.05 | 0.23 | 0.84±0.09 | 0.158 | 53±5.7 |
| 330 | 1.52±0.08 | 0.29±0.03 | 0.23 | 1.0 ±0.09 | 0.154 | 65±5.8 |
| 400 | 1.29±0.07 | 0.29±0.05 | 0.23 | 0.77±0.10 | 0.141 | 55±7 |
| $q^2=20.0$ F$^{-2}$ | | | | | | |
| 250 | 0.52±0.04 | 1.14±0.08<br>(0.22±0.13)[a] | 0.15 | 0.15±0.13 | 0.151 | 10±9 |
| 330 | 0.97±0.06 | 0.97±0.1<br>(0.47±0.13)[a] | 0.15 | $0.35_{-0.14}^{+0.54}$ | 0.137 | $26_{-10}^{+39}$ [b] |

[a] Corrected for meson contamination.
[b] Upper limit set by letting $\sigma^+=0$.

## VIII. DATA

A list of the data obtained is given in Tables III–VII. All energies are expressed in MeV and cross sections in units of $10^{-35}$ cm$^2$/sr MeV. The column labeled WAB is the calculated value for the wide-angle bremsstrahlung. Errors on $\sigma^-$ and $\sigma^+$ are errors from counting statistics only. No over-all absolute error was included, because the comparison with form factors derived from elastic scattering, also used for the normalization in this experiment, automatically compensates this error, except to provide an over-all multiplicative uncertainty in all nucleon form factors. The columns labeled "$\sigma^-$" and "$\sigma^+$" correspond to the cross sections for negative and positive settings of the spectrometer and have already had several minor corrections mentioned above applied. $\Gamma'_{\text{transverse}}$ is calculated from formula (5) but with $K$ replaced by $\mathbf{K}_{\text{lab}}$. A suitable change was made in the calculation of $\sigma_{\text{transverse}}$. Figures 4–7 show graphically the experimental data, the consistency with the assumption of negligible longitudinal transition currents, and with currently assumed values for the nucleon form factors.

## IX. INTERPRETATION

Upon replacing $\mathbf{K}$ by $\mathbf{K}_{\text{lab}}$ in $\Gamma$ (denoted by $\Gamma'$), one obtains

$$\frac{d^2\sigma}{d\Omega d\epsilon'}=\Gamma'_{\text{transverse}}\int d\Omega_{Q^*}\frac{d\sigma}{d\Omega^*},$$

where $Q^*$ is the magnitude of the meson momentum in the center of mass frame.

$$\frac{d\sigma}{d\Omega^*}=\frac{1}{64\pi^2}\frac{Q^*}{|\mathbf{K}|^*}\sum_{\substack{\text{spins,}\\ \text{polarization}}}|\langle\mathbf{J}_T\rangle|^2.$$

($|\mathbf{K}|^*$ is the center-of-mass *momentum* of the virtual photon, and $E$ is total center of mass energy.) With this definition of $\Gamma'$ and $\sigma$, two factors of $M/E$ can be absorbed into the transition current matrix elements $\mathbf{J}_T$, and $\mathbf{J}_T$ evaluated in the center-of-mass system (one of the $M/E$ factors comes from the final-state phase space), which agrees with the definition of $\mathbf{J}$ by CGLN and FNW. An alternative not followed here might be to use the photoproduction ($q^2=0$) center-of-mass momentum $K^*=(M/E)K$ in the definition of $d\sigma/d\Omega$, corresponding to the use of $\Gamma$ instead of $\Gamma'$. The present choice offsets some purely kinematic variation of the matrix elements with $q^2$. The summation is extended over photon polarizations and initial and final nuclear spins. Although the virtual photon is polarized, the integration over meson angles in the final state makes this separation possible, as was stated in Sec. III above and discussed in refer-

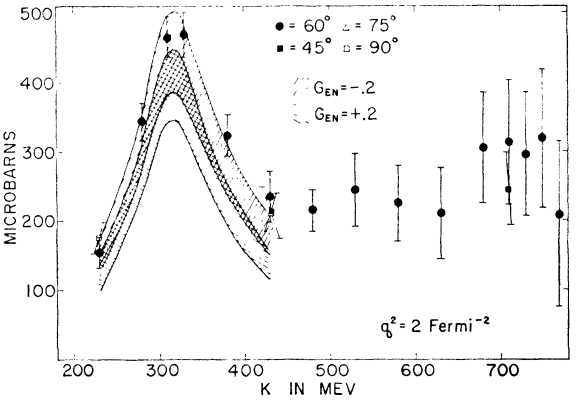


FIG. 4. Total cross sections for pion electroproduction.

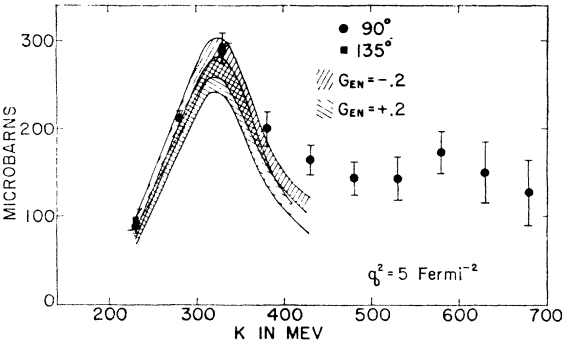


FIG. 5. Total cross sections for pion electroproduction.

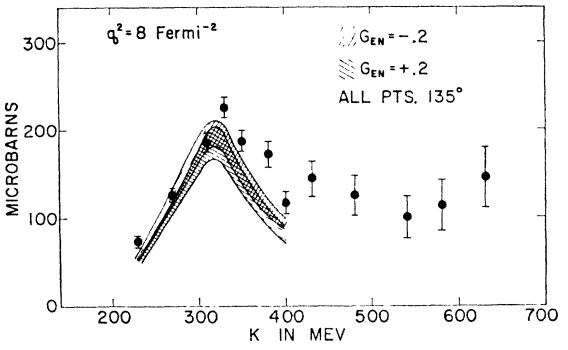


FIG. 6. Total cross sections for pion electroproduction.

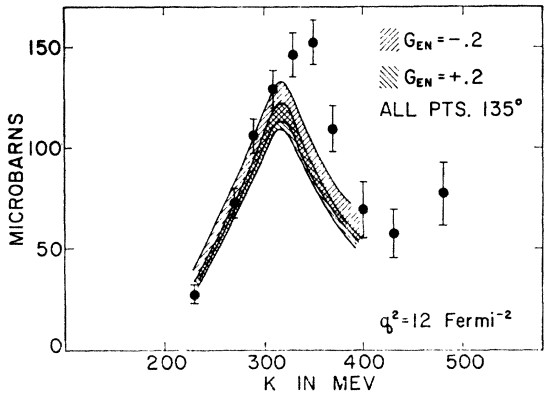


FIG. 7. Total cross sections for pion electroproduction.

ence 16. This is equivalent to the statement that no interference is observed between matrix elements corresponding to angular momentum change along the direction of momentum transfer of 0, +1 or −1 units.

An expression for $J_T$ was given in terms of form factors and phase shifts in FNW and discussed in the paper by Gartenhaus and Lindner.[14] After squaring the matrix element, summing over spins and integrating over meson directions, one obtains an expression for $\sigma_{\text{transverse}}$ which is essentially a quadratic form in the various nucleon form factors, with a dependence on $K$ given by kinematic factors from the various multipoles and by the energy variation of the pion-nucleon phases. The pion current (retardation) term was multiplied by "$F_\pi$", although strictly speaking, this is not quite the pion form factor, since one of the pions is virtual and hence some $K$ dependence might appear in this factor. Thus, we may express the cross section in terms of ten numbers, representing the coefficients of $F_\pi^2$, $F_\pi G_{En}$, etc., all at constant $q^2$. When $F_\pi$ was treated as a variable, the total cross section was quite insensitive to values of $F_\pi$ between 0 and 1, the variation being a few percent. There was slightly more sensitivity on either side of the resonance peak than at $K=320$ MeV. The theoretical matrix element is expected to be incorrect to order $q^2/M^2$, and two changes were made in order to approximate the unknown correction terms:

1. The replacement $F_1 \rightarrow G_E$. $G_E$ corresponds to spin-independent absorption of the virtual photon, and it seems likely on physical grounds that $s$-wave pion production involves $G_E$ rather than $F_1$. The difference is of order $q^2/2M^2$, which is negligible for $q^2<12$ F$^{-2}$, compared to the uncertainty in $G_{En}$.

2. The $p$-wave amplitudes $h^{++}$, $h^{--}$, $h^{+-}$, and $h^{-+}$ were multiplied by the factor $(1+q^2/2M^2)^{-1/2}$ which had the effect of decreasing the amplitude for large $q^2$. Fubini *et al.* suggest this factor as an approximate correction for large $q^2$. At $q^2=2$ F$^{-2}$, the square of the resonant amplitude is thus decreased 5%. Omission of this term would lessen the discrepancy between a choice of positive $G_{En}$ and the experimental results.

For each value of $q^2$ where extensive data are available, the pion electroproduction cross section was calculated for center-of-mass energies ranging from $K=230$ MeV to $K=450$ MeV. Figure 8 is a comparison of the $\pi^0$ and $\pi^+$ total cross sections with the theory using the experimental phase shifts given in Table VIII. An empirical fit was used for the $S$-wave phases given by Pontecorvo[26]:

$$\delta_1=0.17Q^*,$$
$$\delta_3=-0.085Q^*\ (1+0.154Q^{*2}).$$

Values for the $P$-wave phases were estimated from smoothed fits to the analysis given by Dietz and

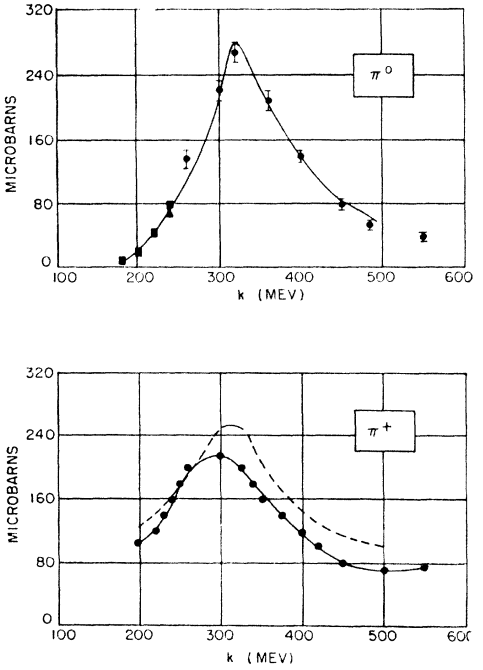


FIG. 8. Theoretical fit to total cross sections for single-pion photoproduction. Experimental pion-nucleon phase shifts are used.

[26] B. Pontecorvo, *Ninth Annual International Conference on High-Energy Physics, Kiev, 1959* (Academy of Sciences, Moscow, 1960); J. Hamilton, and W. S. Woolcock, Phys. Rev. **118**, 291 (1960).

Hohler.[27] Using $f^2=0.081$, the fit to the $\pi^0$ photoproduction total cross section agrees almost perfectly with the experimental data,[28] but the experimental cross section for $\pi^+$ photoproduction is 10–15% below the theoretical prediction. The source of this discrepancy is not known, but it appears that it cannot be ascribed to use of the $1/M$ expansion by CGLN, since recoil corrections are equally large for $\pi^0$ photoproduction and seem properly accounted for when the matrix element is constrained to the phase it must possess by virtue of the final state theorem. Of course, a total cross section is the weakest test of the theory, since interference with residual amounts of $d$ wave, etc., averages to zero in the total cross section. Nevertheless, the fit to the $\pi^0$ data so obtained contains no adjustable parameters, i.e., only pion-nucleon scattering data is used in obtaining it.

The bands in Figs. 4–7 represent the limits of uncertainty in the predicted pion electroproduction cross section due to the uncertainty in $G_{Ep}$, $G_{Mp}$, and $G_{Mn}$,

TABLE VIII. Smoothed experimental values used for pion-nucleon phase shifts (in degrees).

| $K$ (MeV) | $\delta_{11}$ | $\delta_{13}$ | $\delta_{31}$ | $\delta_{33}$ |
|---|---|---|---|---|
| 160 | 0 | 0 | 0 | 0 |
| 175 | −0.4 | −0.25 | −0.4 | 2.3 |
| 200 | −1.2 | −0.5 | −1.2 | 6.55 |
| 225 | −1.6 | −0.75 | −1.6 | 12.7 |
| 250 | −2.0 | −1.0 | −2.0 | 22.5 |
| 275 | −1.75 | −1.25 | −2.5 | 35.8 |
| 300 | −1.5 | −1.5 | −3.0 | 52.5 |
| 325 | 0.1 | −1.75 | −3.7 | 84.0 |
| 350 | 1.8 | −2.0 | −4.5 | 102.5 |
| 375 | 3.6 | −2.25 | −5.2 | 112.0 |
| 400 | 5.4 | −2.5 | −6.0 | 120.0 |
| 425 | 6.7 | −2.75 | −7.2 | 127.5 |

as determined from proton elastic and deuteron quasi-elastic scattering. It was necessary to consider in some detail the error correlations between the $G$'s obtained in elastic scattering experiments. The numerical values of the $G$'s as taken from the data reported by Hofstadter and collaborators[1,2] are plotted in Fig. 9 in terms of $G_{Ep}^2$, etc. The squares of the $G$'s are given because these are the actual measured quantities, and to emphasize the lack of knowledge about $G_{En}^2$. The errors on the $G$'s were assigned in the following manner:

(a) First, it is assumed that a straight-line fit of the form $A+B\cot^2(\theta/2)$ is made for each $q^2$ at 2, 5, 8, 12 F$^{-2}$. Although the data do not correspond to exactly these values of the momentum transfer, only points

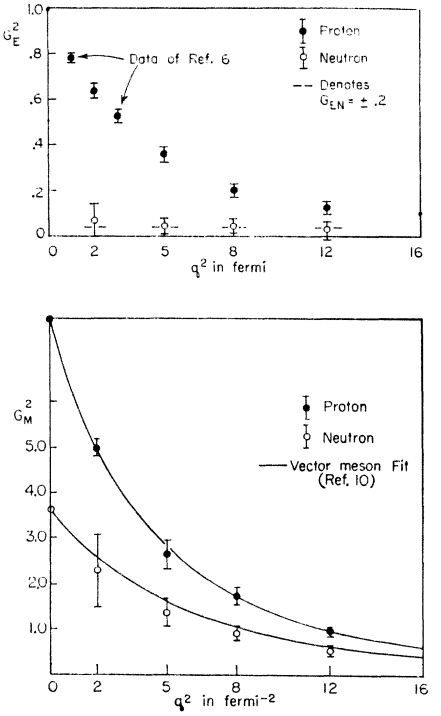


FIG. 9. Values and approximate errors assigned to the nucleon helicity form factors.

within 2 F$^{-2}$ of the desired $q^2$ were used in estimating the error on the $G$'s and no additional error was assigned for the interpolation, it being assumed, that in each case the error was as quoted in reference 1. From the two-by-two matrix formed by the second derivatives of $\chi^2$ for the straight line fit at some particular value of $q^2$, it is possible, by matrix inversion, to obtain the expected standard deviations of $A$ and $B$ from their mean values $\bar{A}$, $\bar{B}$ determined by the least-squares linear fit, as well as the expected correlation between deviations of $A$ and $B$ from the mean values. This is commonly represented in terms of an "error ellipse", which is the curve of constant probability for deviations from the mean in $(A,B)$ space. It proves convenient for this application to work with the principal axes of this ellipse, which can be treated as independent random variables—most conveniently normalized so that these particular linear combinations of $A$-$\bar{A}$ and $B$-$\bar{B}$ have a mean expectation value of zero and an rms expectation value of one.

In terms of these variables, denoted by $\xi_1$ and $\xi_2$, a particular value of $A$-$\bar{A}$ and $B$-$\bar{B}$, or equivalently $G_E^2$ and $G_M^2$ may be written:

$$G_E^2=(G_E^2)_{\rm av}+\alpha\xi_1+\beta\xi_2$$
$$G_M^2=(G_M^2)_{\rm av}+\gamma\xi_1+\delta\xi_2.$$

$\alpha$, $\beta$, $\gamma$, $\delta$ are functions of the experimental points and their errors, as derived in the manner indicated above. We may obtain the variances of the above or any linear combination and their correlations in terms of expecta-

[27] K. Dietz and G. Hohler, Z. Naturforsch. **14a**, 995 (1959); and Z. Physik **157**, 362 (1959). These also agree substantially with those reported by B. Pontecorvo and others in the Kiev Conference Notes (1960).

[28] $\pi^0$ experimental data: R. G. Vasil'kev, B. B. Govorkov, and V. I. Gol'danskii, Soviet Phys.—JETP **37**, 7 (1960); W. S. McDonald, V. Z. Peterson, and D. R. Corson, Phys. Rev. **107**, 577 (1957); L. Koester and F. Mills, *ibid.* **105**, 1900 (1957). $\pi^+$ experimental data: average of existing data as summarized by F. Dixon [Ph.D. thesis, California Institute of Technology, 1960 (unpublished)].

tion values of $\xi_1$ and $\xi_2$. For example:

$$\langle[G_E{}^2-(G_E{}^2)_{\rm av}]^2\rangle=\alpha^2\langle\xi_1{}^2\rangle+2\alpha\beta\langle\xi_1\xi_2\rangle+\beta^2\langle\xi_2{}^2\rangle$$
$$=\alpha^2+\beta^2.$$

The errors plotted in Fig. 9 for $G_{Ep}{}^2$ correspond to $\pm(\alpha^2+\beta^2)^{1/2}$. If the error is much less than the most probable value $(G^2)_{\rm av}$, then we may also write a similar expression for $G$, where $\alpha$ and $\beta$ become multiplied by $1/(2G)$. All information about form factor error correlations is thus contained in $\alpha$, $\beta$, $\gamma$, $\delta$. It is important to treat these correlations properly to avoid a completely erroneous impression of the sensitivity of the pion electroproduction to neutron structure and to the errors on the proton form factors as determined by elastic scattering.

(b) Next, using the above error coefficients, we calculate the smoothed Rosenbluth cross section and associated error for the points at which quasi-elastic scattering data from the deuteron are available. From the knowledge of $R=(\sigma_p+\sigma_n)/\sigma_p$ as measured by experiment and the calculated smoothed $\sigma_p$ we may obtain $\sigma_n\pm\Delta\sigma_n$ and thereupon repeat the process in part (a) for $G_{En}{}^2$ and $G_{Mn}{}^2$. The error on $R$ includes both experimental errors in the ratio and an error due to theoretical uncertainties in deriving $\sigma_n+\sigma_p$ from the measured cross section. $\Delta R/R$ was assigned to be 5% for all $q^2$ except $q^2=2$, where a 10% uncertainty was assigned due to the increased final-state interaction correction. The error on $\sigma_n$ is a combination of the error on $\sigma_p$ and on $R$. It should be emphasized that the values of the $G$'s are those taken from smooth curves through the values of $F_1$ and $F_2$ found by Hofstadter and collaborators—only the error correlations have been estimated.

(c) It is then a simple matter to calculate the range of uncertainty in the pion electroproduction from these numbers. As explained above, this analysis is not especially meaningful for $G_{En}$, and only the dependence on the constant values $+0.2$ and $-0.2$, both allowed by the quasi-elastic data, is shown in Figs. 4–7.

To summarize, it might be said that pion electroproduction is in fair agreement with the current experimental picture of nucleon structure, but that favoritism is exhibited by the data for negative $G_{En}$. The interaction leading to pion production is demonstrated to proceed via transverse currents, and the FNW factorization of final-state interactions and nucleon structure effects is valid for low $q^2$, but begins to break down for $q^2\geq 8$ F$^{-2}$, as manifested in the upward shift of the resonance peak at large $q^2$. Negative $G_{En}$ would be in contradiction with the neutron-electron interaction and dispersion relations, unless small amounts of a low-mass state ($\approx m_\pi$), normally excluded, were present.[10] Upper limits on $\sigma_{\rm scalar}/\sigma_{\rm transverse}$ can be established to be about 35% for $q^2=2$, $k=230$, 430 MeV, 35% for $q^2=5$, $K=230$ MeV, and 25% for $q^2=5$, $K=330$ MeV. Better sensitivity to $\sigma_{\rm scalar}/\sigma_{\rm transverse}$ could easily be obtained with better statistical accuracy and a wider range of $\theta$.

## ACKNOWLEDGMENTS

We wish to thank Professor W. K. H. Panofsky for his encouragement and advice, and E. A. Allton for many helpful discussions. R. Alvarez, M. Bazin, and D. Coward helped take data. Excellent performance of the linear accelerator at very high energies was ensured by the work of the accelerator crew under G. Gilbert.